A tumor-suppressor function for NFATc3 in T-cell lymphomagenesis by murine leukemia virus

Sys Zoffmann Glud, Annette Balle Sørensen, Mindaugas Andrulis, Bruce Wang, Eisaku Kondo, Randi Jessen, Laszlo Krenacs, Eva Stelkovics, Matthias Wabl, Edgar Serfling, Alois Palmetshofer, and Finn Skou Pedersen

Nuclear factor of activated T cell (NFAT) transcription factors play a central role in differentiation, activation, and elimination of lymphocytes. We here report on the finding of provirus integration into the *Nfatc3* locus in T-cell lymphomas induced by the murine lymphomagenic retrovirus SL3-3 and show that NFATc3 expression is repressed in these lymphomas. The provirus insertions are positioned close to the *Nfatc3* promoter or a putative polyadenylated RNA (polyA) region. Furthermore, we demonstrate that NFATc3-deficient mice infected with SL3-3 develop T-cell lymphomas faster and with higher frequencies than wild-type mice or NFATc2-deficient mice. These results identify NFATc3 as a tumor suppressor for the development of murine T-cell lymphomas induced by the retrovirus SL3-3. (Blood. 2005;106:3546-3552)

Introduction

The family of nuclear factor of activated T cell (NFAT) transcription factors comprises the 5 structurally related proteins NFATc1, c2, c3, and c4, whose activity is controlled by Ca^{++} signals, and NFAT5, which is controlled by osmotic stress. All NFAT proteins contain a DNA binding domain of approximately 300 amino acids (aa), which, due to its similar conformation to the Rel domain of nuclear factor κB (NF-κB) factors, is designated as Rel similarity domain (RSD).[1-3] NFATc1 expression is inducible in lymphocytes, while NFATc2 and NFATc3 are constitutively expressed. They regulate lymphocyte development, and upon antigen receptor stimulation they control both the initiation and activation of immune responses, and antigen-induced cell death (AICD) of lymphocytes. In resting cells, NFAT proteins are highly phosphorylated and reside in cytoplasm. Antigen receptor triggering leads to increasing intracellular concentrations of free Ca^{++}, which activate the Ca^{++}/calmodulin-dependent protein phosphatase calcineurin (CN). The activity of CN results in nuclear translocation of NFATs and activation (or repression) of numerous NFAT target genes. In T cells, NFAT transcription factors control the expression of many immunomodulatory genes including the cytokines interleukin-2 (IL-2), IL-4, IL-5, IL-13, and interferon γ (IFNγ); the surface receptors CD25 and Fas ligand (FasL); and also genes that are involved in cell-cycle regulation.[1-3]

Through the inactivation of *Nfatc,* genes in mice both individual and overlapping activities have been detected for the genes encoding *Nfatc1, c2,* or *c3*.[1-3] Whereas inactivation of *Nfatc1* and *c2* genes results in a general loss of lymphokine production,[4] T helper 2 (Th2)–type lymphokines are overexpressed in mice deficient for NFATc2[5] and are much more pronounced in mice double deficient for NFATc2 and NFATc3.[6] These results indicate that the NFAT factors NFATc1, c2, and c3 play an essential role in differentiation of naive Th cells to Th effector cells. In addition, NFATc3 is shown to control the transition of developing thymocytes from the $CD4^+CD8^+$ double-positive (DP) stage to the mature $CD4^+CD8^-$ or $CD4^-CD8^+$ single-positive (SP) stages.[7] Mice lacking NFATc3 show an impaired development of CD4 and CD8 SP thymocytes, and the resulting thymic defect is characterized by increased apoptosis of DP thymocytes.[7]

Retrovirus insertional mutagenesis in mouse models has helped to identify a variety of genetic loci that are directly or indirectly contributing to the processes of tumor induction and progression.[8] The data obtained from various retroviral insertion tagging studies (http://rtcgd.ncifcrf.gov/index.html) as well as our own results include several cases of retroviral integrations within the *Nfatc1*[9] and *Nfat5* loci, suggesting that deregulation of these NFAT proteins may contribute to retrovirus-induced cancerogenesis.

Using a model of T-cell lymphoma induction by the T-cell lymphomagenic retrovirus SL3-3, in combination with paternal ENU (*N*-ethyl-*N*-nitrosourea) mutagenesis, we here report the finding of 3 provirus insertions into the *Nfatc3* locus, located within the *Nfatc3* promoter and close to a putative proximal polyadenylated RNA (polyA) region. In all 3 cases, virus insertion resulted in a repression of NFATc3 expression. To address the effect of NFATc3 expression in lymphomagenesis, we infected wild-type mice and

From the Department of Molecular Biology, University of Aarhus, Aarhus, Denmark; the Department of Molecular Pathology, Institute of Pathology, University of Wuerzburg, Wuerzburg, Germany; Picobella, Burlingame, CA; the Department of Pathology, Okayama University Graduate School of Medicine and Dentistry, Okayama, Japan; the Laboratory of Tumor Pathology and Molecular Diagnostics, Institute of Biotechnology, Bay Zoltan Foundation for Applied Research, Szeged, Hungary; the Department of Microbiology and Immunology, University of California, San Francisco, CA; and the Department of Medical Microbiology and Immunology, University of Aarhus, Aarhus, Denmark.

Submitted February 7, 2005; accepted July 8, 2005. Prepublished online as *Blood* First Edition Paper, July 28, 2005; DOI 10.1182/blood-2005-02-0493.

Supported by grants from the Danish Cancer Society, the Danish Research Agency, Karen Elise Jensen's Fund, The Mildred-Scheel-Stiftung for Cancer Research, The Wilhelm Sander Stiftung, the German Science Foundation (DFG), and the National Institutes of Health (US) (grant AG20684).

A.P. and F.S.P. contributed equally to this work.

Reprints: Finn Skou Pedersen, Department of Molecular Biology, University of Aarhus, C. F. Møllers Allé, Bldg 130, DK-8000 Aarhus C, Denmark; e-mail: fsp@mb.au.dk.

The publication costs of this article were defrayed in part by page charge payment. Therefore, and solely to indicate this fact, this article is hereby marked "advertisement" in accordance with 18 U.S.C. section 1734.

mice deficient for NFATc3 (or NFATc2) with SL3-3 and investigated the generation of retrovirally induced tumors and mortality. We found that NFATc3, but not NFATc2, exerts a repressive effect on both incidence and latency periods of tumor induction. This indicates a tumor suppressor role of NFATc3 for the generation of T-cell lymphomas induced by the retrovirus SL3-3.

Materials and methods

Screening for SL3-3 insertions

A large panel of T-cell lymphomas induced by the NB-tropic SL3-3 murine leukemia virus (MLV) in wild-type BALB/c mice was analyzed for provirus integration sites by anchored polymerase chain reaction (PCR).[10] Virus-infected mice were offspring from crossing males treated with ENU (doses, 3×20 mg/kg or 3×100 mg/kg body weight) with nontreated females. ENU is a chemical germ-line mutagen, which, in combination with insertional mutagenesis from infectious retroviruses, potentially increases the chances of detecting tumor suppressor genes by retroviral tagging.[11]

In 3 tumors from 3 different mice, provirus insertions at the following positions in the *Nfatc3* locus (NM_010901) were found: 5′-ATATATTTGCTATTCCTCTCTCTCTCAACCCTGATGGGAGACTATCTCT**G**-provirus-3′ (chromosome [Chr] 8 105372659); 5′-GGAGGAGGTGGTCACTGGCTTCTCCCAACTCCTTCTCTTAATCATGCGC**T**-provirus-3′ (Chr 8 105372946); and 5′-provirus-**G**TTTTGTCTTTTCATTTTGAGACGGGGAAGGGCTCACTCTGTAGCTGGCC-3′ (Chr 8 105419363). (The first 50 bases of genomic sequence that follow immediately after the virus 5′ long terminal repeat [LTR] are given. The base marked in bold is the first base after the virus 5′ LTR; that is, the given chromosome position. See also Figure 1A.)

Mice

Offspring from an initial breeding setup with crosses of *Nfatc2*$^{+/-}$*Nfatc3*$^{+/-}$ mice as well as crosses of *Nfatc2*$^{-/-}$*Nfatc3*$^{+/-}$ males with female wild-type BALB/c mice were used for further breeding. One-hundred and seventy-four newborn (< 36 hours old) BALB/c mice were inoculated intraperitoneally with wild-type NB-tropic SL3-3 MLV particles (described in Thomas et al[13] and kindly provided by Christopher Y. Thomas), with an additional 70 newborn BALB/c control mice mock-injected with complete medium. At the time of weaning, tail clips were used for genotyping. The mice were monitored every day for a period of 250 days for signs of disease development (weight loss, breathing difficulties, bristly fur, inactivity, or tumor development; diagnosed on the basis of gross appearance of lymphoid organs). When sickness was registered, the mice were killed by cervical dislocation. Spleen, thymus, liver, and lymph nodes were dissected and measured, and samples were immediately frozen at −80°C. Samples from a representative number of mice from each genotypic group were analyzed by flow cytometry. Mouse breeding and housing was performed at Pipeline Biotech, Denmark.

Tumors

Tumors were diagnosed on the basis of enlargement of lymphoid organs. Based on the size of thymus and spleen in 7 healthy, mock-infected, age-matched mice and on previously used guidelines in SL3-3 studies,[14] the following measures were used to consider the lymphoid organs that were enlarged and tumor bearing: spleen, 30 mm or longer; mesenteric lymph node, 20 mm or longer; and thymus and lymph nodes other than mesenteric, 10 mm or wider/longer.

Flow cytometry

Single cells from minced tissues were washed with RPMI medium (Gibco, Invitrogen, Taastrup, Denmark), and erythrocytes were lysed by incubating in 0.16 M NH_4Cl, 1 mM $NaHCO_3$, and 0.12 mM EDTA (ethylenediaminetetraacetic acid) on ice for 5 minutes and then adding 1 volume of 0.12 M NaCl, 17 mM Na-citrate. Per sample, 1×10^6 trypan blue excluding cells were incubated with anti–mouse CD16/CD32 (Fcγ III/II receptor, Mouse Fc block; BD Pharmingen, Bröndby, Denmark) and then with antibodies (BD Pharmingen) staining T cells (CD3–phycoerythrin [PE], CD4–fluorescein isothiocyanate [FITC], CD8α–peridinin chlorophyll-α protein [PerCP]–cyanine 5.5 [Cy5.5]), B cells (B220-PerCP), or myeloid cells (CD11b-FITC), or immunoglobulin (Ig) isotype controls. Appropriate isotype controls were done in parallel. Flow cytometry was performed on a fluorescence-activated cell sorter (FACS) Calibur apparatus (BD Bioscience, San Jose, CA) with a single 15-mM air-cooled Argon laser tuned at 488 nm. Data analysis, including compensation of overlapping spectra of the antibodies, was performed by use of WinList 3D (version 5.0; Verity Software House, Topsham, ME).

Tissue processing and immunohistochemistry

Paraffin sections were cut and stained either for hematoxylin and eosin (H&E) or were used for immunohistochemical staining, following wet heat–induced antigen retrieval. B-cell–, T-cell–, and myeloid cell–associated antigens were detected using monoclonal antibodies and polyclonal rabbit antibodies cross-reactive with mouse, including monoclonal anti-CD79a (Labvision, Fremont, CA) and anti–TIA-1/GMP-17 (granule membrane protein of 17 kDa) (Immunotech, Miami, FL) as well as polyclonal anti–terminal deoxyribonucleotidyl transferase (TdT; DaKoCytomation, Carpinteria, CA), antimyeloperoxidase (Labvision), anti-CD3ϵ, and biotinylated anti–mouse IgM (DaKoCytomation).

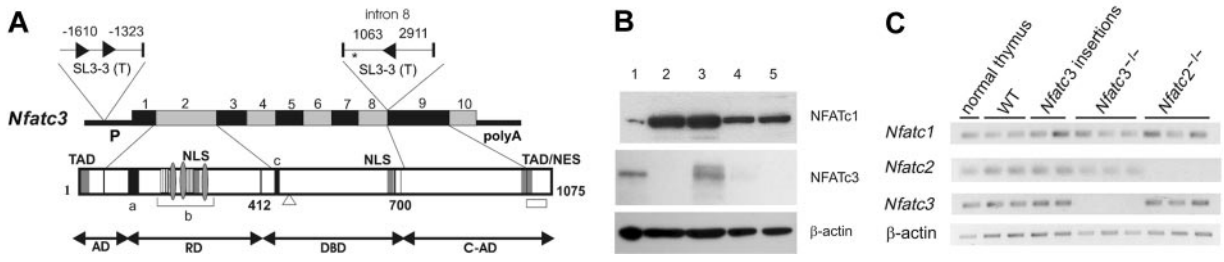

Figure 1. Insertion of retrovirus SL3-3 in the *Nfatc3* locus represses NFATc3 expression. (A) Schematic representation of *Nfatc3* with SL3-3 MLV insertion sites and orientations indicated by arrowheads (▶). The numbers adjacent to the proviruses denote the distance (in bp) between provirus insertions and the upstream and downstream exons or the distance between neighboring insertions. TAD indicates transactivation domain; NLS, nuclear localization signal; a, calcineurin binding site; b, region within the regulatory domain (RD) containing multiple phosphorylation sites; c, the DNA-binding motif in the DNA-binding domain (DBD); TAD/NES, combinatorial C-terminal TAD (TAD-C) and nuclear export signal found in NFATc1 and NFATc3; □, the alternative 33-aa sequence of the NFATx2 isoform of NFATc3[12] lacking TAD-C motif; △, the 30-aa deletion of an inactive isoform of NFATc3[12]; and *, location of a putative polyA site (AATAAATAGTCTTTTTT) in NFATc3 with start at position chr8:105418773. (B) Western blot analysis of protein extracts from lymphomas with SL3-3 insertion within the *Nfatc3* locus using polyclonal anti-NFATc1 or anti-NFATc3 antibody for staining ("Materials and methods"). Protein extracts from normal thymus of a wild-type mouse (lane 1) are compared with lysates from tumors of *Nfatc3*$^{-/-}$ (lane 2) or wild-type mice without (lane 3) and with (lanes 4 and 5, representing tumors with insertion in intron 8 and at 1.6-kb upstream, respectively) SL3-3 MLV insertion at the *Nfatc3* locus. (C) RNA expression of NFAT genes in SL3-3–induced tumors as determined by semiquantitative RT-PCR. Shown are the expression in normal thymus, thymic tumors derived from wild-type, *Nfatc2*$^{-/-}$-, and *Nfatc3*$^{-/-}$ mice, and thymic tumors with provirus insertion in *Nfatc3* locus (at intron 8 and 1.6-kb upstream). cDNA amounts were equalized to β-actin signals. WT indicates wild type.

Acetone-fixed frozen tumor sections were incubated with a mixture of Alexa-488–conjugated anti–mouse CD4, Alexa-647–conjugated anti–mouse CD8 (both from Caltag, Burlingame, CA), and biotinylated anti-CD3, followed by incubation with streptavidine-Cy3 (both from BD Pharmingen). Finally, nuclei were stained with DAPI (4,6 diamidino-2-phenylindole; Sigma, St Louis, MO). Immunofluorescent signals were captured using confocal laser scanning microscopy (software version 2.5; Leica, Heidelberg, Germany).

RT-PCR

Semiquantitative reverse-transcriptase (RT)–PCR was performed using RNA extract from normal thymus and thymic tumors. Total RNA (3 μg) was reverse transcribed using RevertAid H Minus First Strand cDNA Syntheses Kit (Fermentas, Hanover, MD). Standard PCR was done using 150 ng or 6 ng RNA equivalent of cDNA for NFATc3 and β-actin, respectively, for 25 cycles. For NFATc1, touchdown PCR was done for 20 cycles followed by standard PCR for 20 cycles. For NFATc2, touchdown PCR was done for 14 cycles followed by standard PCR for 30 cycles. Primers used for detecting *Nfatc1*, *Nfatc2*, *Nfatc3*, and β-actin are as follows: nfatc1s, 5′-atgccaagcaccagctttccagtcccttcc-3′; nfatc1as, 5′-gcccgctgtccacagcccctccgta-3′; nfatc2s, 5′-cctcacgggccag aacttcacagcg-gagtcc-3′; nfatc3as, 5′-cctctttccgttgatgacgtagaagttgac-3′; nfatc3s, 5′-ccaggtgcatcggattactgg-3′; nfatc3as, 5′-tcgctgagagcactcaacagg-3′; β-actins, 5′-tcaacaccccagccatgtacgtagccatcc-3′; and β-actins, 5′-tgtagacgaccttccacctgt-3′.

Western blotting

For detecting NFATc1 or NFATc3, 30 μg protein per lane was electrophoresed through 8% polyacrylamide (PAA) gels and immunodetected with polyclonal anti-NFATc1 and anti-NFATc3 antibody (sc-8321; Santa Cruz Biotechnology, Santa Cruz, CA) followed by visualization using the enhanced chemiluminescence (ECL) system (Amersham, Arlington Heights, IL). To confirm equal protein loading, membranes were stripped and subsequently incubated with an anti–β-actin antibody (sc-8432; Santa Cruz).

Results

Extinction of NFATc3 expression by proviral insertion in T-cell lymphomas

In a large-scale study of retroviral tagging in SL3-3–induced T-cell lymphomas of 1767 mice, we found 3 specific provirus insertions in the *Nfatc3* gene in 3 independent tumors, out of a total of 6514 mapped provirus tags from all the tumors. Two of the insertion sites in *Nfatc3* are located within the 5′ promoter region at positions 1.3 kb and 1.6 kb upstream of exon 1. The third provirus integration site is positioned in intron 8, that is, 1063 base pairs (bp) downstream of exon 8 and, therefore, 589 bp downstream of a putative proximal polyA site (Figure 1A). Of interest, these regions are homologous to regions in which provirus insertions have been found for the *Nfatc1* gene[9,15,16] and that appear to control NFATc1 expression ("Discussion"). The latencies of tumor development in mice with provirus insertion in the *Nfatc3* gene (81, 85, and 98 days) were similar to those of the complete study group (84 ± 30 days).

To investigate the effects of provirus insertions on NFATc3 expression, we performed Western blots using protein extracts from tumors harboring insertions in the *Nfatc3* gene locus. In these assays, we found no detectable NFATc3 protein expression (Figure 1B). The repression of protein expression, however, showed by semiquantitative RT-PCR not to be paralleled by a similar repression of *Nfatc3* mRNA expression (Figure 1C). Likewise, the expression of the genes *Nfatc2* and *Nfatc1* as well as NFATc1 protein was not affected by the presence NFATc3 repression in the tumors (Figure 1B-C). The tumor with provirus insertion 1.3-kb upstream of *Nfatc3* demonstrated low-quality RNA (presumably because it was not retrieved immediately after death) and was therefore left out of the RT-PCR assay and the Western blot. The repression of NFATc3 expression in the tumors led us to assume that NFATc3 may act as a tumor suppressor for the SL3-3–induced lymphomagenesis and prompted us to study lymphomagenesis in NFATc3-deficient mice.

Enhanced disease incidence and shorter latency in NFATc3-deficient mice

To study the role of NFATc3 and of the related NFATc2 in oncogenesis, newborn BALB/c mice, as well as BALB/c mice homozygous or heterozygous for inactivated *Nfatc2* or *Nfatc3* genes, were inoculated intraperitoneally with the T-cell lymphomagenic retrovirus SL3-3 MLV. Disease incidence and latency periods were monitored for an observation period of 250 days. Since no major differences with regard to disease incidence, tumor phenotype, and latency were observed for animals with homozygous deletion of either *Nfatc2* or *Nfatc3* harboring 1 or 2 wild-type alleles of the complementary *Nfat* gene, 3 groups of animals were compared: $Nfatc2^{-/-}$, $Nfatc3^{-/-}$, and those with wild-type *Nfatc2* and *c3* genes (including double heterozygotes, $Nfatc2^{+/-}c3^{+/-}$). $Nfatc2^{-/-}c3^{-/-}$ mice remained unconsidered due to the severe phenotype they develop, as described previously.[17]

Virus-infected $Nfatc3^{-/-}$ mice developed disease with 100% incidence, and with the exception of 2 animals, all mice showed significantly enlarged thymus, and many of them also had enlarged spleen and mesenteric lymph nodes (Table 1). The calculated mean latency of the $Nfatc3^{-/-}$ mice was 81 ± 21 days. In contrast, the disease incidence in the group of wild-type animals was 83% after an average latency period of 92 ± 44 days (Table 1). The shorter latency for SL3-3–induced disease in $Nfatc3^{-/-}$ mice compared with their wild-type littermates ($Nfatc3^{+/+}$ and $Nfatc3^{+/-}$) is significant ($P = .026$) according to the log-rank testing. The disease incidence of the $Nfatc2^{-/-}$ mice was found to be 91%, with an average latency period of 109 ± 47 days. Taking into consideration that disease incidence is not 100% in either the wild-type group or the $Nfatc2^{-/-}$ group, the slightly longer average latency of $Nfatc2^{-/-}$ mice is not significantly different from that of wild-type

Table 1. Disease and lymphoma development in SL3-3—infected BALB/c mice

Genotype	Virus	Disease incidence, % (no./total)	Lymphoma incidence,* % (no./total)	Mean latency, d ± std†
WT	SL3-3	80 (8/10)	70 (7/10)	88 ± 32
$Nfatc2^{+/-}$ $c3^{+/-}$	SL3-3	83 (40/48)	65 (31/48)	93 ± 45
$Nfatc2^{+/+}$ $c3^{-/-}$	SL3-3	100 (6/6)	100 (6/6)	80 ± 8
$Nfatc2^{+/-}c3^{-/-}$	SL3-3	100 (10/10)	80 (8/10)	83 ± 23
$Nfatc2^{-/-}$ $c3^{+/+}$	SL3-3	93 (38/41)	63 (26/41)	108 ± 51
$Nfatc2^{-/-}$ $c3^{+/-}$	SL3-3	89 (42/47)	60 (28/47)	110 ± 43
Pooled genotypes				
WT	SL3-3	83 (48/58)	66 (38/58)	92 ± 44
WT	Mock	19 (4/21)	10 (2/21)	112 ± 60
$Nfatc3^{-/-}$	SL3-3	100 (16/16)	88 (14/16)	81 ± 21
$Nfatc3^{-/-}$	Mock	10 (1/10)	0 (0/10)	45‡
$Nfatc2^{-/-}$	SL3-3	91 (80/88)	60 (53/88)	109 ± 47
$Nfatc2^{-/-}$	Mock	61 (11/18)	17 (3/18)	116 ± 63

Std indicates standard deviation.

*Based on clear enlargement of lymphoid organs as described in "Materials and methods."

†Mean latency is calculated for disease-developing mice.

‡Only one mouse in the group developed disease; number indicates its lifespan.

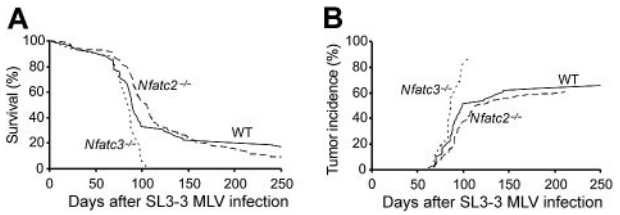

Figure 2. Diminished survival and increased tumor incidence in *Nfatc3*$^{-/-}$ mice after SL3-3 infection. (A) Survival curves of *Nfatc3*$^{-/-}$ (n = 16/16), *Nfatc2*$^{-/-}$ (n = 80/88), or wild-type (n = 48/58) (including heterozygotes) BALB/c mice infected with SL3-3. (B) The cumulative incidence of tumor development of *Nfatc3*$^{-/-}$ (n = 14/16), *Nfatc2*$^{-/-}$ (n = 53/88), and wild-type (n = 38/58) mice based on enlarged lymphoid organs as defined previously (for details, see "Materials and methods").

mice ($P = .85$), which is also reflected in the survival curves for the 2 groups (Figure 2A). Among mock-infected control mice, only those with inactivated *Nfatc2* gene showed a considerable number of disease-developing mice (11 of 18), of which 3 presented with significantly enlarged organs, an observation consistent with the previously published phenotype.[18]

Focusing only at clear enlargement of lymphoid organs, lymphoma incidence was lower than disease incidence in all pooled genotype groups. Lymphoma incidence was markedly higher among *Nfatc3*$^{-/-}$ mice, with 14 (88%) of 16 mice showing significantly enlarged organs in comparison with wild-type and *Nfatc2*$^{-/-}$ mice having lymphoma incidences of 66% and 60%, respectively (Table 1; Figure 2B).

SL3-3 induces similar tumors in both wild-type and NFATc3-deficient mice

The finding that mice bearing homozygous inactivation of the *Nfatc3* gene have a shorter latency for SL3-3–induced T-cell lymphoma than those with either defective *Nfatc2* gene or wild-type *Nfat* genes supports the notion that NFATc3, but not NFATc2, exerts a tumor-suppressor function for SL3-3–induced tumors.

To address if the loss of NFATc3 (or of NFATc2) had any influence on disease specificity, the tumors were examined by staining sections with H&E, or with various antibodies raised against extracellular or intracellular markers. A typical feature of the tumors, irrespective of the tumor tissue or *Nfat* genotype, is, as shown in Figure 3A, a lymphomateous infiltrate composed of medium-sized monotonous tumor cells with prominent mitotic activity. The cells display rather dispersed chromatin structure and relatively low nuclear-cytoplasm ratio, suggesting that the tumor cells are of an early differentiation state. Most of the cases analyzed revealed a strong membranous immunostaining for CD3ε and no staining for myeloperoxidase (MPO, some positive signal due to the presence of body macrophages, Figure 3A), TIA-1, CD79a, and IgM (data not shown), indicating that the tumor cells are of T-cell or NK-cell origin. Several cases revealed TdT-positive tumor cells (Figure 3A), which adds further evidence to a precursor T-cell origin of the tumors.[19] Additional phenotypic characterization of the differentiation state of the T cells revealed different tumor

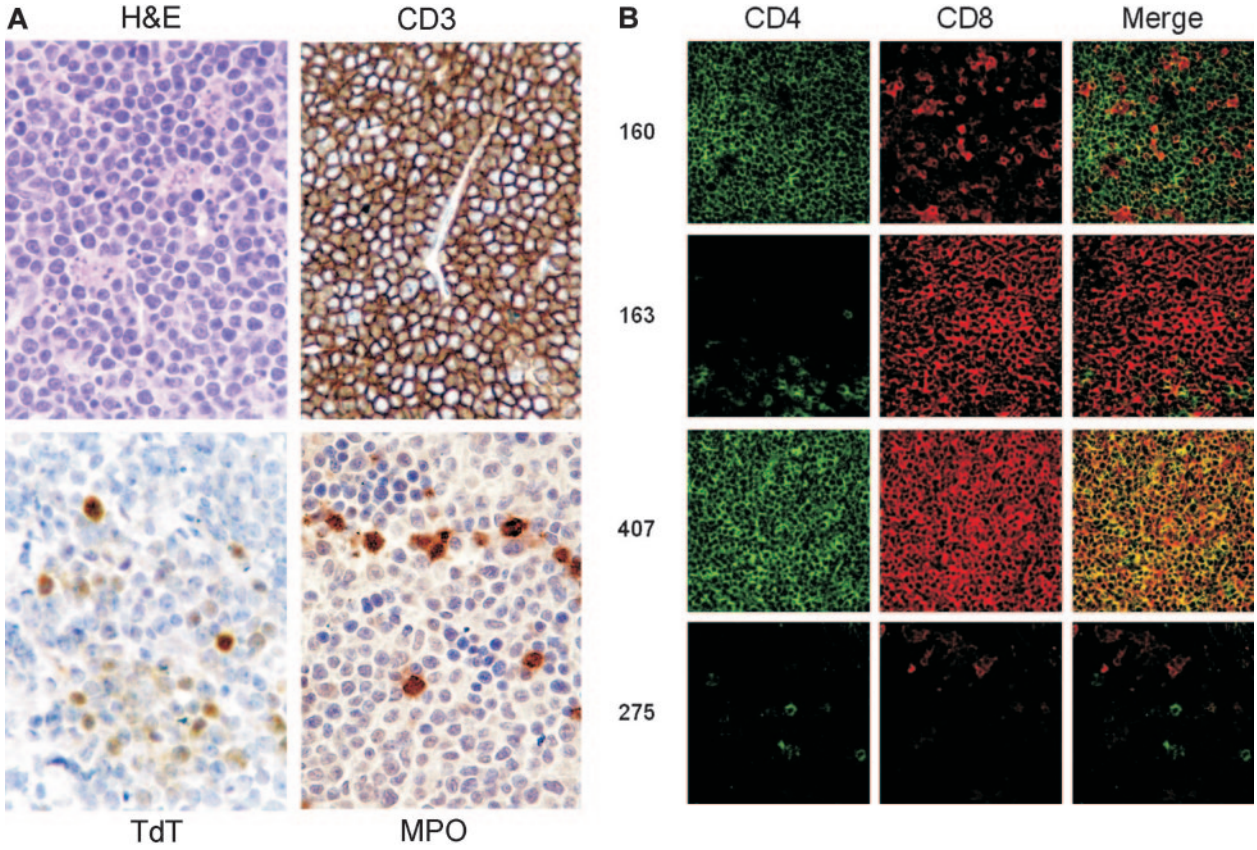

Figure 3. Immunohistochemical analyses of SL3-3–induced tumors. (A) Sections of a representative tumor of the thymus stained with either H&E or antibodies against CD3ε (CD3), TdT, and myeloperoxidase (MPO). (B) Immunohistochemical stainings of CD3ε^{+} tumors from different animals for double fluorescent analysis of CD4 and CD8 expression. All of the samples shown were either CD3ε bright (nos. 160, 163, 407 all thymus) or CD3ε dim (no. 275; mesentery lymph node). The genotypes of the mice with the tumors shown are *Nfatc3*$^{-/-}$ (nos. 160, 163, 407) and *Nfatc2*$^{-/-}$ (no. 275). Images were acquired with Leica TCS SP2 Confocal System equipped with a Leica DMRE microscope with an HCX PL APO 40×/1.25 NA oil CS objective lens. Images were processed with Leica Confocal Software version 2.61 (all from Leica Microsystems, Mannheim, Germany).

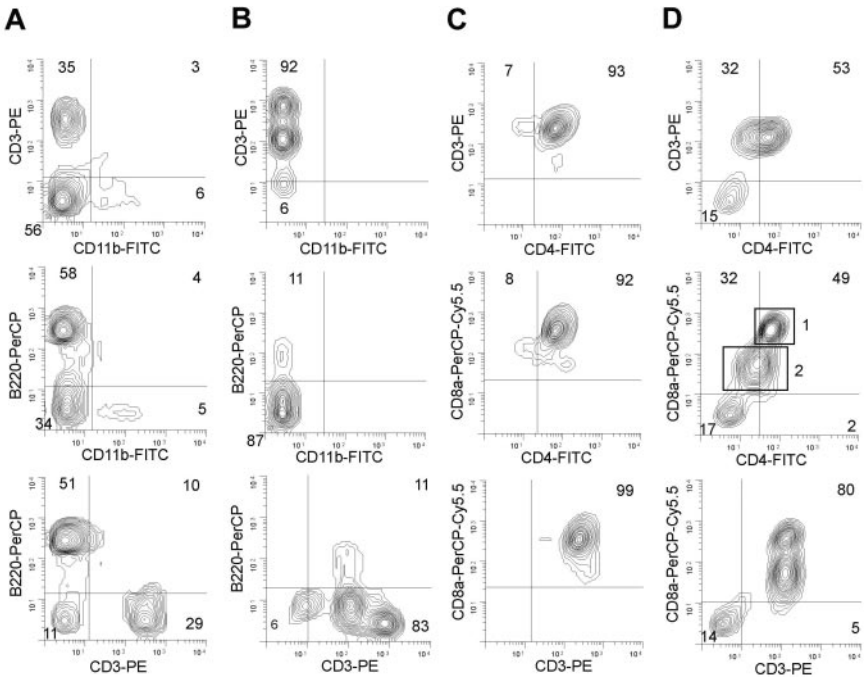

Figure 4. SL3-3 infection leads to various subtypes of T-cell lymphomas in wild-type and NFATc2- or NFATc3-deficient mice. Flow cytometry analysis of cells from (A) spleen of mock-infected *Nfatc3*$^{-/-}$ mice, (B) spleen lymphoma from a SL3-3–infected *Nfatc3*$^{-/-}$ mouse, (C) thymus lymphoma from an SL3-3–infected wild-type mouse, and (D) spleen lymphoma from an SL3-3–infected *Nfatc2*$^{-/-}$ mouse. (A-B) To distinguish between T cells, myeloid cells, and B cells, cells were stained with a mixture of anti-CD3–PE, anti-CD11b–FITC, and anti-CD45/B220–PerCP Abs, respectively. In panels C and D, a mixture of anti-CD3–PE, anti-CD4–FITC, and anti-CD8–PerCP–Cy5.5 antibodies was used to distinguish among T-cell subtypes. Two different populations of T cells in panel D are indicated with rectangles 1 and 2 representing CD3$^+$CD4$^+$CD8$^+$ cells and CD3$^+$CD4$^{-(dim)}$CD8$^{+(dim)}$ cells, respectively. Note that parallel analysis of both thymus and spleen tumors derived from the same animal revealed basically identical FACS profiles in most of the cases investigated. Five percent probability contour plots are shown. Grids are positioned according to background fluorescence of isotype controls. Numbers in quadrants indicate the percentage of cells within the limits of the quadrants. For a summary of tumor phenotypes, see Table 2.

phenotypes of either mature CD4$^+$ or CD8$^+$ SP cells or immature CD4$^+$CD8$^+$ DP cells (Figure 3B).

Staining of cells from 45 tumors from either wild-type, *Nfatc2*$^{-/-}$, or *Nfatc3*$^{-/-}$ mice with antibodies binding to T cells (anti-CD3–PE), B cells (anti-B220–PerCP), and myeloid cells (anti-CD11b–FITC) showed that regardless of tumor tissue and *Nfat* genotype, all analyzed lymphomas (n = 45) were clearly CD3$^+$ T-cell lymphomas. Whereas healthy thymuses and spleens from mock-infected, age-matched, control mice contained 75% to 85% and 30% to 50% of CD3$^+$ cells, respectively, the lymphomagenic thymuses and spleens of virus-infected mice had up to 15% and 50% higher levels of CD3$^+$ cells, respectively (Figure 4A-B).

Further characterization of T-cell subsets using anti-CD4 and anti-CD8 antibodies revealed a heterogeneous pattern of phenotypes, giving no clear correlation between either the lymphoid tissue (thymus, lymph node, or spleen) analyzed or the *Nfat* genotype (Table 2). Most of the lymphomas (38 of 49) contained one dominant cell type. However, 2 equally large populations dominated in 11 lymphomas (Table 2); 9 lymphomas of which were characterized as having a CD4$^+$CD8$^+$ DP/CD8$^+$ SP mixed phenotype (Figure 4D), probably reflecting oligoclonal tumors. Among tumors with one dominant population, a major group of lymphomas (22 of 38, of which 9 tumors were analyzed by immunohistochemistry) was characterized by a large population containing immature T cells. Tumor cells from 5 of these 22 tumors showed a phenotype of immature CD4$^-$CD8$^-$ double-negative (DN) cells, whereas the remaining 17 tumors were of the immature CD4$^+$CD8$^+$ DP phenotype (Table 2; Figures 3B-4C), a cell type normally present only in the thymic cortex prior to differentiation into either CD4$^+$ SP or CD8$^+$ SP T-cell subsets. In addition, lymphomas of mature CD4$^+$ SP or mature CD8$^+$ SP phenotypes were found, albeit with slightly lower frequencies than those with an immature T-cell phenotype (Table 1).

To prove the T-cell origin of tumors, DNA was investigated for genetic rearrangements at the T-cell receptor β (TCR-β) and Igκ chain loci in Southern blots.[14] In 39 lymphoid tumors (from 17 mice), no rearrangements of Igκ locus were found, whereas all contained rearrangements of either the TCR-$J_{\beta1}$ or the TCR-$J_{\beta2}$ gene segments, or of both (data not shown), supporting a clonal (or oligoclonal) origin of T-cell lymphomas.

Table 2. Lymphoma phenotypes induced upon SL3-3 MLV infection

Phenotype	Total	WT	*Nfatc2*$^{-/-}$	*Nfatc3*$^{-/-}$
One dominant phenotypic cell population	38*	NA	NA	NA
Immature CD4$^-$CD8$^-$ DN	5	2	3	0
Immature CD4$^+$CD8$^+$ DP	17	8	3	6
Mature CD4$^-$CD8$^+$ SP	8	3	2	2
Mature CD4$^+$CD8$^-$ SP	8	6	1	2
Two dominant phenotypic cell populations	11†	NA	NA	NA
CD4$^+$CD8$^+$DP / CD4$^-$CD8$^+$ SP	9	3	4	2
CD4$^+$CD8$^+$DP / CD4$^+$CD8$^-$	2	0	1	1

NA indicates not applicable.
*Nine of these 38 tumors were analyzed by immunohistochemistry.
†Two of these 11 tumors were analyzed by immunohistochemistry.

Discussion

Retroviral insertional mutagenesis in laboratory mice provides a powerful tool to identify cancer-relevant genes. As a result of infecting mice that either express proto-oncogenic transgenes or harbor homozygous deletions of particular genes, the relevance of partially redundant gene products with regard to cancerogenesis can be further defined.[15,20,21] Here, we report on insertions of T-cell lymphomagenic retrovirus SL3-3 MLV into the *Nfatc3* locus in 3 independent T-cell lymphomas of a total of 1767 mice screened. Due to the randomness of provirus integration, the finding of 3 such hits defines the nfatc3 locus as a common insertion site (CIS) and indicates the presence of a cancer-associated gene.[20] Furthermore, we show that these insertions are associated with repression of NFATc3 protein level, while the *Nfatc3* RNA level is similar to

normal thymus and control tumors. In these tumors, only one allele of the *Nfatc3* gene is targeted by the provirus. Hence, the lack of protein must involve posttranscriptional mechanisms. We cannot, however, exclude an additional transcriptional repression effect at either the provirus-targeted or untargeted, possibly ENU-mutated, allele. Irrespective of the mechanisms, the association of provirus insertion with repression of the NFATc3 protein level in the 3 tumors suggests that abrogation of NFATc3 expression provides the cell with a survival and/or proliferation advantage.

In addition to the *Nfatc3* insertions, the 3 tumors also contained provirus insertions into other noncommon retroviral insertion sites as well as insertions at the frequently targeted oncogenes Myc and Myb. How NFATc3 protein repression may cooperate with these other insertional mutations in lymphomagenesis must await further studies.

The provirus insertions in *Nfatc3* are positioned at comparable sites of provirus insertions found in *Nfatc1* (Mouse Retrovirus Tagged Cancer Gene Database[40] and data not shown). In either *Nfatc* locus, the provirus insertions cluster in or close to the promoter region, implicating an important functional role of viral insertions in regulation of NFAT expression. Likewise, the insertions near the 3′ end of both genes appear to cluster at or near polyA addition sites. This is true for the *Nfatc1* gene where several insertions were found in intron 10 (Mouse Retrovirus Tagged Cancer Gene Database[40] and data not shown), that is, within the last intron, located just 5′ from the short exon 11, which harbors the strong distal polyA site.[22] The 3′ insertion next to exon 8 in *Nfatc3* (Figure 1A) seems to be located near a putative proximal poly A site. This conclusion is supported by the generation of short NFATc3 isoforms (designated as NFAT4a and NFAT4b by Hoey et al[23]), which are similar in length to NFATc1/A. This short NFATc1 isoform is synthesized by the use of a proximal, inducible polyA site, which has been described to terminate exon 9 of *Nfatc1* gene (which is homologous to exon 8 of *Nfatc3*).[24,25]

Comparing SL3-3 MLV–induced lymphomagenesis in wild-type, *Nfatc2*$^{-/-}$, and *Nfatc3*$^{-/-}$ BALB/c mice, we obtained support for a tumor-suppressor function of NFATc3. Virus-infected NFATc3-deficient mice develop lymphomas with a significantly shorter latency period and at a much higher frequency than both wild-type and NFATc2-deficient mice. The tumor phenotypes induced, however, did not differ among the different *Nfatc2/3* genotypes. Phenotypically, a major proportion of tumors were found to be derived from immature $CD4^-CD8^-$ DN or $CD4^+CD8^+$ DP thymocytes. This finding is consistent with previous studies of SL3-3–accelerated lymphomas in AKR mice.[26,27] In contrast, inbred NMRI mice primarily develop lymphomas of the mature $CD3^+CD4^+CD8^-$ SP T-helper cell phenotype upon infection with SL3-3.[13]

It was interesting to note that SL3-3–infected *Nfatc2*$^{-/-}$ mice are markedly less prone to lymphoma induction compared with *Nfatc3*$^{-/-}$ mice. Part of the explanation for this difference might be due to the different importance of NFATc2 and NFATc3 in thymocytes. During thymocyte development, NFAT members are expressed at varying levels and NFATc3 is most abundantly expressed at the $CD4^+CD8^+$ DP stage of thymocyte differentiation.[28,29] A constitutively active form of NFATc3 was recently shown to induce the differentiation of $CD4^+CD8^+$ DP lymphocytes to mature SP T cells, whereas other NFAT proteins appear to be more important in maturation of peripheral lymphocytes.[30] Mice lacking NFATc3 show an impaired development of $CD4^+$ and $CD8^+$ SP thymocytes and peripheral T cells. In addition, the thymic defect is characterized by increased apoptosis of $CD4^+CD8^+$ DP thymocytes.[7] Similar to NFATc2, NFATc3 acts in a proapoptotic manner in peripheral T cells, whereas in thymus, NFATc3 appears to promote the survival of thymocytes by regulating Bcl-2 and FasL expression. Earlier studies suggest that initial SL3-3 virus infection and cell transformation evolve in the immature thymocytes and induce thymic atrophy.[26,27,31,32] Hence, the higher lethality of $CD4^+CD8^+$ DP thymocytes in *Nfatc3*$^{-/-}$ mice may increase the chances of the virus to induce thymic atrophy, providing space for the expansion of truly malignant cells escaping the normal selection process in thymus. In part, this may explain the higher risk of lymphoma development in *Nfatc3*$^{-/-}$ mice compared with wild-type and *Nfatc2*$^{-/-}$ mice. Nevertheless, the loss of NFATc3 expression by provirus tagging, in the 3 SL3-3–induced tumors, demonstrates that loss of function of NFATc3 also at the level of a single-cell clone can provide an infected cell with a selective advantage in provirus-induced transformation.

Until now, a direct involvement of NFAT factors in lymphomagenesis has not been demonstrated. Due to aberrant chondrocyte development in NFATc2-deficient mice, NFATc2 was suggested to represent a tumor suppressor for the development of cartilagous tumors,[33] whereas a constitutively active version of NFATc1/A behaves like an oncoprotein by inducing a transformed phenotype upon ectopic expression in 3T3-L1 fibroblasts.[34] Our results presented here and the proapoptotic activity of several NFAT proteins, including NFATc2 and c3,[22,35-37] suggest that several NFAT proteins can act as tumor suppressors for the development of lymphoid tumors in mice. It remains to be shown whether this might also hold true for human tumors.

A large study of gene expression profiles from human B-cell lymphomas included expression analysis of both NFATc1 and NFATc3.[38] By searching the online supplementary Lymphoma/Leukemia Molecular Profiling Project (LLMPP) microarray datasets,[41] we did not detect remarkable changes in expression levels of NFATc3 in numerous samples from patients with lymphoma. In contrast, NFATc1 expression was found to be low or mildly expressed in follicular B-cell lymphoma, reduced in chronic lymphocytic lymphoma (B-CLL), and markedly reduced in several transformed lymphoma cell lines. In the majority of diffuse large B-cell lymphomas (DLBCLs), NFATc1 expression was reduced or low (except for 3 samples in which expression was as high as in normal T cells). Our own histochemical stainings of a large panel of human lymphomas demonstrate that in human anaplastic large cell lymphomas (ALCLs) and in classic Hodgkin lymphomas NFATc1 expression is suppressed, in most cases due to the epigenetic silencing of *Nfatc1* promoter region by DNA methylation (A. Akimzhanov, L.K., S. Klein-Hessling, E. Stelkovics, E. Bagdi, E.K., T. Schlegel, S. Chupvilo, T. Rüdiger, H. K. Müller-Hermelink, A.P., and E. Serfling, manuscript submitted). These findings suggest that similar to the related NF-κB proteins,[39] NFAT proteins control the development and progression of various types of human lymphomas and, possibly, of other tumors, and therefore, exert both oncogenic and tumor-suppressive activities depending on the specific cellular context.

Acknowledgments

We wish to thank Petra Sprosty and Julia Burghardt for excellent technical assistance; Dr Laurie Glimcher (Boston) for kindly providing mice with inactivated *Nfatc2* and *Nfatc3* alleles; and Alexander Schmitz for help with flow cytometry analysis.

References

1. Serfling E, Berberich-Siebelt F, Chuvpilo S, et al. The role of NF-AT transcription factors in T cell activation and differentiation. Biochim Biophys Acta. 2000;1498:1-18.
2. Crabtree GR, Olson EN. NFAT signaling: choreographing the social lives of cells. Cell. 2002; 109(suppl 2):S67-S79.
3. Hogan PG, Chen L, Nardone J, Rao A. Transcriptional regulation by calcium, calcineurin, and NFAT. Genes Dev. 2003;17:2205-2232.
4. Peng SL, Gerth AJ, Ranger AM, Glimcher LH. NFATc1 and NFATc2 together control both T and B cell activation and differentiation. Immunity. 2001;14:13-20.
5. Xanthoudakis S, Viola JP, Shaw KT, et al. An enhanced immune response in mice lacking the transcription factor NFAT1. Science. 1996;272:892-895.
6. Ranger AM, Oukka M, Rengarajan J, Glimcher LH. Inhibitory function of two NFAT family members in lymphoid homeostasis and Th2 development. Immunity. 1998;9:627-635.
7. Oukka M, Ho IC, de la Brousse FC, Hoey T, Grusby MJ, Glimcher LH. The transcription factor NFAT4 is involved in the generation and survival of T cells. Immunity. 1998;9:295-304.
8. Akagi K, Suzuki T, Stephens RM, Jenkins NA, Copeland NG. RTCGD: retroviral tagged cancer gene database. Nucleic Acids Res. 2004;32: D523-D527.
9. Sorensen AB, Duch M, Amtoft HW, Jorgensen P, Pedersen FS. Sequence tags of provirus integration sites in DNAs of tumors induced by the murine retrovirus SL3–3. J Virol. 1996;70:4063-4070.
10. Mikkers H, Allen J, Knipscheer P, et al. High-throughput retroviral tagging to identify components of specific signaling pathways in cancer. Nat Genet. 2002;32:153-159.
11. Breuer M, Slebos R, Verbeek S, van Lohuizen M, Wientjens E, Berns A. Very high frequency of lymphoma induction by a chemical carcinogen in pim-1 transgenic mice. Nature. 1989;340:61-63.
12. Liu J, Koyano-Nakagawa N, Amasaki Y, et al. Calcineurin-dependent nuclear translocation of a murine transcription factor NFATx: molecular cloning and functional characterization. Mol Biol Cell. 1997;8:157-170.
13. Thomas CY, Nuckols JD, Murphy C, Innes D. Generation and pathogenicity of an NB-tropic SL3–3 murine leukemia virus. Virology. 1993;193: 1013-1017.
14. Sorensen KD, Quintanilla-Martinez L, Kunder S, Schmidt J, Pedersen FS. Mutation of all Runx (AML1/Core) sites in the enhancer of T-lymphomagenic SL3–3 murine leukemia virus unmasks a significant potential for myeloid leukemia induction and favors enhancer evolution toward induction of other disease patterns. J Virol. 2004; 78:13216-13231.
15. Suzuki T, Shen H, Akagi K, et al. New genes involved in cancer identified by retroviral tagging. Nat Genet. 2002;32:166-174.
16. Hansen GM, Skapura D, Justice MJ. Genetic profile of insertion mutations in mouse leukemias and lymphomas. Genome Res. 2000;10:237-243.
17. Ranger AM, Oukka M, Rengarajan J, Glimcher LH. Inhibitory function of two NFAT family members in lymphoid homeostasis and Th2 development. Immunity. 1998;9:627-635.
18. Hodge MR, Ranger AM, Charles de la Brousse F, Hoey T, Grusby MJ, Glimcher LH. Hyperproliferation and dysregulation of IL-4 expression in NF-ATp-deficient mice. Immunity. 1996;4:397-405.
19. Morse HC III, Anver MR, Fredrickson TN, et al. Bethesda proposals for classification of lymphoid neoplasms in mice. Blood. 2002;100:246-258.
20. Lund AH, Turner G, Trubetskoy A, et al. Genome-wide retroviral insertional tagging of genes involved in cancer in Cdkn2a-deficient mice. Nat Genet. 2002;32:160-165.
21. Mikkers H, Allen J, Knipscheer P, et al. High-throughput retroviral tagging to identify components of specific signaling pathways in cancer. Nat Genet. 2002;32:153-159.
22. Chuvpilo S, Jankevics E, Tyrsin D, et al. Autoregulation of NFATc1/A expression facilitates effector T cells to escape from rapid apoptosis. Immunity. 2002;16:881-895.
23. Hoey T, Sun YL, Williamson K, Xu X. Isolation of two new members of the NF-AT gene family and functional characterization of the NF-AT proteins. Immunity. 1995;2:461-472.
24. Chuvpilo S, Avots A, Berberich-Siebelt F, et al. Multiple NF-ATc isoforms with individual transcriptional properties are synthesized in T lymphocytes. J Immunol. 1999;162:7294-7301.
25. Chuvpilo S, Zimmer M, Kerstan A, et al. Alternative polyadenylation events contribute to the induction of NF-ATc in effector T cells. Immunity. 1999;10:261-269.
26. Hays EF, Bristol GC, McDougall S, Klotz JL, Kronenberg M. Development of lymphoma in the thymus of AKR mice treated with the lymphomagenic virus SL 3-3. Cancer Res. 1989;49:4225-4230.
27. Hays EF, Bristol G. Observations on lymphomagenesis and lymphoma in AKR mice: a description of prelymphoma changes in the thymus and phenotypic diversity of lymphomas induced by SL3–3 virus. Thymus. 1992;19:219-234.
28. Ho SN, Thomas DJ, Timmerman LA, Li X, Francke U, Crabtree GR. NFATc3, a lymphoid-specific NFATc family member that is calcium-regulated and exhibits distinct DNA binding specificity. J Biol Chem. 1995;270:19898-19907.
29. Amasaki Y, Miyatake S, Arai N, Arai K. Regulation of nuclear factor of activated T-cell family transcription factors during T-cell development in the thymus. J Allergy Clin Immunol. 2000;106:S1-S9.
30. Amasaki Y, Adachi S, Ishida Y, et al. A constitutively nuclear form of NFATx shows efficient transactivation activity and induces differentiation of CD4(+)CD8(+) T cells. J Biol Chem. 2002; 277:25640-25648.
31. Rulli K, Lenz J, Levy LS. Disruption of hematopoiesis and thymopoiesis in the early premalignant stages of infection with SL3–3 murine leukemia virus. J Virol. 2002;76:2363-2374.
32. Hays EF, Bristol GC, Lugo JP, Wang XF. Progression to development of lymphoma in the thymus of AKR mice treated neonatally with SL 3-3 virus. Exp Hematol. 1989;17:1116-1121.
33. Ranger AM, Gerstenfeld LC, Wang J, et al. The nuclear factor of activated T cells (NFAT) transcription factor NFATp (NFATc2) is a repressor of chondrogenesis. J Exp Med. 2000;191:9-22.
34. Neal JW, Clipstone NA. A constitutively active NFATc1 mutant induces a transformed phenotype in 3T3-L1 fibroblasts. J Biol Chem. 2003;278: 17246-17254.
35. Youn HD, Chatila TA, Liu JO. Integration of calcineurin and MEF2 signals by the coactivator p300 during T-cell apoptosis. EMBO J. 2000;19: 4323-4331.
36. Rengarajan J, Mittelstadt PR, Mages HW, et al. Sequential involvement of NFAT and Egr transcription factors in FasL regulation. Immunity. 2000;12:293-300.
37. Kondo E, Harashima A, Takabatake T, et al. NF-ATc2 induces apoptosis in Burkitt's lymphoma cells through signaling via the B cell antigen receptor. Eur J Immunol. 2003;33:1-11.
38. Alizadeh AA, Eisen MB, Davis RE, et al. Distinct types of diffuse large B-cell lymphoma identified by gene expression profiling. Nature. 2000;403: 503-511.
39. Karin M, Cao Y, Greten FR, Li ZW. NF-kappaB in cancer: from innocent bystander to major culprit. Nat Rev Cancer. 2002;2:301-310.
40. National Cancer Institute. Retrovirus Tagged Gene Database. http://rtcgd.nciferf.gov/index.html. Accessed June 2004.
41. Lymphoma/Leukemia Molecular Profiling Project. http://llmpp.nih.gov/lymphoma. Accessed October 2004.